sciendo

Polish Journal of Medical Physics and Engineering
The Journal of Polish Society of Medical Physics
ISSN 1898-0309, doi: 10.2478/pjmpe-2020-0028

December 2020
Vol 26, Issue 4

Scientific Paper

# Determination of effective source to surface distance and cutout factor in small fields in electron beam radiotherapy: A comparison of different dosimeters

Mohamad Reza BAYATIANI[a], Fatemeh FALLAHI[b], Akbar ALIASGHARZADEH[b], Mahdi GHORBANI[c], Benyamin KHAJETASH[d], Fatemeh SEIF[a,*]

[a]*Medical Physics and Radiotherapy Department, School of Paramedical Sciences, Arak University of Medical Sciences and Ayatollah Khansari Hospital, Arak, Iran*

[b]*Department of Medical Physics, School of Paramedical Sciences, Kashan University of Medical Sciences, Kashan, Iran*

[c]*Biomedical Engineering and Medical Physics Department, School of Medicine, Shahid Beheshti University of Medical Sciences, Tehran, Iran*

[d]*Medical Physics Department, School of Medicine, Iran University of Medical Sciences, Tehran, Iran*

[*]*E-mail address: seif@arakmu.ac.ir*

## Abstract

*Objective:* The main purpose of this study is to calculate the effective source to surface distance ($SSD_{eff}$) of small and large electron fields in 10, 15, and 18 MeV energies, and to investigate the effect of SSD on the cutout factor for electron beams a linear accelerator. The accuracy of different dosimeters is also evaluated.

*Materials and methods:* In the current study, Elekta Precise linear accelerator was used in electron beam energies of 10, 15, and 18 MeV. The measurements were performed in a PTW water phantom (model MP3-M). A Semiflex and Advanced Markus ionization chambers and a Diode E detector were used for dosimetry. $SSD_{eff}$ in 100, 105, 110, 115, and 120 cm SSDs for $1.5 \times 1.5$ cm$^2$ to $5 \times 5$ cm$^2$ (small fields) and $6 \times 6$ cm$^2$ to $20 \times 20$ cm$^2$ (large fields) field sizes were obtained. The cutout factor was measured for the small fields.

*Results:* $SSD_{eff}$ in small fields is highly dependent on energy and field size and increases with increasing electron beam energy and field size. For large electron fields, with some exceptions for the $20 \times 20$ cm$^2$ field, this quantity also increases with energy. The $SSD_{eff}$ was increased with increasing beam energy and field size for all three detectors.

*Conclusion:* The $SSD_{eff}$ varies significantly for different field sizes or cutouts. It is recommended that $SSD_{eff}$ be determined for each electron beam size or cutout. Selecting an appropriate dosimetry system can have an effect in determining cutout factor.

**Key words**: radiotherapy; linac; electron beam; effective SSD; cutout; dosimetry

## Introduction

Electrons are usually used for radiotherapy of superficial tumors at a standard source to surface distance (SSD) of 100 cm. Because of curved and irregular body contours, most patients are treated at extended SSDs. When the treatment is performed at an extended distance, the output of the electron and the percentage depth dose (PDD) must be corrected on the basis of the inverse square law of distance from the source position of the electron. As the electron beam comes out of the accelerator window, it undergoes complex multiple scattering in the scattering foil, the ionization chambers, collimators, the electron applicators, shields at the end of applicators, and the air. The position of the scattering foil cannot be assumed as the nominal source position and the output should be corrected accordingly. In such situations, the output can be accurately predicted using the effective or virtual source location and the inverse square law applied to the effective SSD ($SSD_{eff}$).

The International Commission on Radiation Units and Measurements (ICRU)[1] defines the "virtual point source as a source which when placed in vacuum at some distance $S_{virt}$, that lies away from the scattering foil, will produce electrons which obey the inverse square law, and a mean-square angular spread $\theta^2_{virt}$". For radiation dosimetry and treatment planning purposes with clinical electron beams, accurate knowledge of the location of the virtual source is critical. With changes in the electron gun and the aging condition of the linear accelerator and electron applicators, it is very important to reassess the $SSD_{eff}$.

There are different ways to measure $SSD_{eff}$ such as Full Width at Half Maximum (FWHM), Inverse Slope (IS), and Power Law (PL) methods.[2] The FWHM method is based on measurement of the FWHM of beam profiles, obtained with photographic films used in clinical radiotherapy, as a function of the nominal source to film distance. The IS method is based on dose measurements at small distances between the applicator end and phantom surface (e.g., up to about 20 cm gap). Supposing that $f$ is $SSD_{eff}$, $I_0$ the dose at zero gap, and $I_g$ the dose at gap $g$, then, by plotting the square root of $I_0/I_g$ as function the gap (cm), a straight line is obtained. The slope of this line is $1/(f+d_m)$, and then $f$=(1/slope) – $d_m$ gives the position of the virtual source. The PL method is based on finding an exponent $b$ that fits a power function: $R=a(SSD)+b$. The values of $a$ and $b$ are determined from the least square fitting.[2]

Small cancer lesions are usually treated with electron beams of a linac. For this purpose, electron cutouts can be made customized, based on the tumor size and shape of a specified patient. Dosimetry of such small electron fields should be accurate and includes dosimetric measurement with appropriate dosimeters for small field dosimetry. However, the loss of lateral electronic equilibrium within small fields introduces limitations in accurate dosimetry for such fields.[3] American Association of Physicists in Medicine (AAPM), in the report by Task Group number 25, has recommendations on electron beam dosimetry, especially for small electron fields.[4] Based on this report, due to inherent problems in the existence of electron equilibrium in small electron fields, custom measurements should be performed to determine the change in dose distributions in small electron fields.

Various studies have compared the results of different methods for obtaining $SSD_{eff}$. Jamshidi et al.[5] showed that the measurement of $SSD_{eff}$ using FWHM and multi-pin-hole camera methods have the same results in large field electron beams at an energy greater than 15 MeV. The results of that study have shown that the ISL and PL methods have the same results for all electron energies and field sizes. Al Asmary et al.[6] reported the dependency of $SSD_{eff}$ on the field size and electron beam energy. Their study showed that the results from the ISL and IS methods are consistent. Shafaei Douk et al.[7] showed that the calculated $SSD_{eff}$ values depend on beam energy and field size. For specific energy, the value of $SSD_{eff}$ increases with the increase of field size. Furthermore, for a special applicator, with an increase of electron energy, the value of $SSD_{eff}$ increases. Variation of $SSD_{eff}$ values versus a change of field size in certain energy is more than the variation of $SSD_{eff}$ versus a change of electron energy in certain field size. Tahmasebi Birgani et al.[8] determined the $SSD_{eff}$ of electron beams from a Varian 2100 CD linac. In that study, electron energies of 4, 6, 9, 12, and 15 MeV, electron applicator size of 20 × 20 $cm^2$, nominal SSDs of 97 to 113 cm, and air gaps of 2 cm to 18 cm were studied. Measurements were performed using a 0.13 cc Farmer ionizing chamber. Their results have shown that, in a certain PDD and depth, $SSD_{eff}$ increases with energy.

While different studies have been performed on determination of $SSD_{eff}$ for electron beams, the effect of SSD on cutout factor and the results of $SSD_{eff}$ for different dosimeters have not been evaluated. The aim of this study is to calculate the $SSD_{eff}$ of small and large electron fields at energies of 10, 15, and 18 MeV, and to investigate the effect of SSD on the cutout factor for small fields for a linear accelerator. The accuracy of different dosimeters is also evaluated for the measurement of $SSD_{eff}$.

## Materials and methods

In the current study, $SSD_{eff}$ was determined for an Elekta Precise linear accelerator in electron beam energies of 10, 15, and 18 MeV. $SSD_{eff}$ for 100, 105, 110, 115 and 120 cm SSDs in 1.5 × 1.5, 2 × 2, 2.5 × 2.5, 3 × 3, 3.5 × 3.5, 4 × 4, 4.5 × 4.5, 5 × 5, 6 × 6, 10 × 10, 14 × 14 and 20 × 20 $cm^2$ field sizes were measured. The cutout factor was measured for small electron fields. The measurements were performed in a MP3-M water phantom (PTW, Freiburg, Germany). Semiflex 3D (type 31021) ionization chamber (PTW, Freiburg, Germany), and Advanced Markus electron chamber (PTW, Freiburg, Germany) and Diode E (PTW, Freiburg, Germany) were used for dosimetry. The sensitive volumes of these detectors are 0.07 $cm^3$, 0.02 $cm^3$, and 0.03 $mm^3$, respectively.

The electrometer for reading the detector responses was a UNIDOS E electrometer (PTW, Freiburg, Germany). These detectors were calibrated by a secondary standards dosimetry laboratory (SSDL) which was traceable to the Atomic Energy Organization of Iran (AEOI). The irradiations were performed by 100 monitor units (MUs). Cutouts were placed at the end of the 6 × 6 $cm^2$ applicator. Large fields were also evaluated with 6 × 6 $cm^2$, 10 × 10, 14 × 14, and 20 × 20 $cm^2$ applicators. In this study, the material of cutouts was cerrobend. Cerrobend is a low-melting alloy consisting of tin (13.3%), lead (26.7%), bismuth (50%), and cadmium (10%). The thickness of the cutouts was 1 cm and it was enough to have adequate beam absorption in low and high energy electron beams. The measurements were performed at the Department of Radiotherapy of Ayatollah Khansari Hospital (Arak, Iran).

The maximum depth dose for each energy was obtained using relative dosimetry and then at first, the Diode E detector was placed at the corresponding depth of maximum dose in the phantom to measure absolute dose distribution in different fields. The depth of maximum dose ($d_{max}$) for the energy of 10, 15, and 18 MeV for 10×10 $cm^2$ field were 2.2, 2.51, and 2.72 cm, respectively.

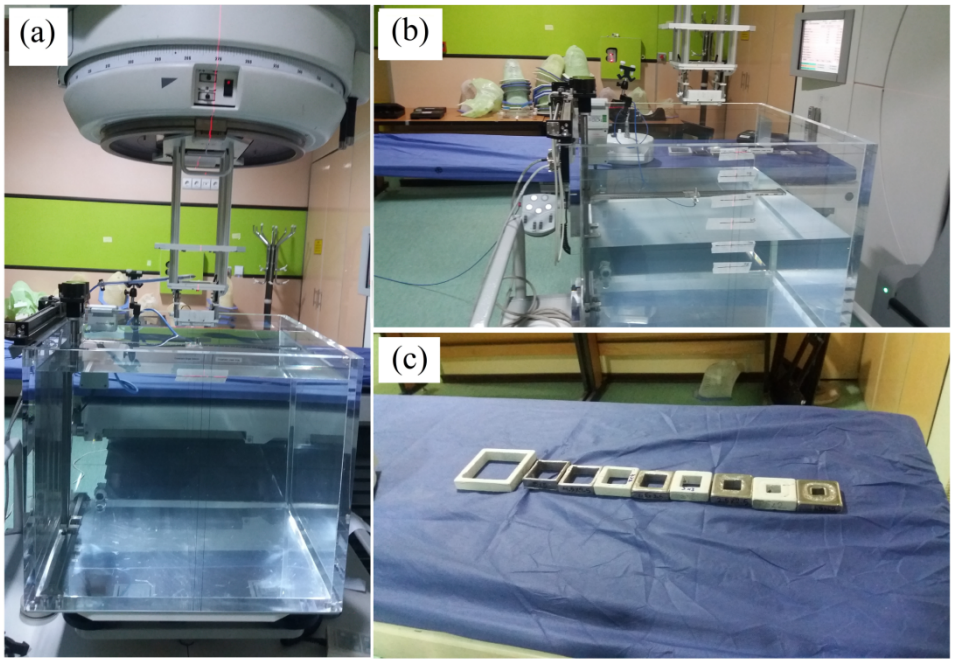


**Figure 1. The setup used for measurements including electron applicator and measuring system (a), different SSDs (b) and used cut outs (c)**

$SSD_{eff}$ in each of the small and large fields was measured at these three energies. The $SSD_{eff}$ was measured by varying the distance of the applicator end to the phantom surface at 100, 105, 110, 115, and 120 cm SSDs with the air gap method.[8] In this method, if $I_0$ is the dose value at a distance of 0 cm and $I_g$ is the dose at a distance of $g$, from the end of the applicator to the phantom surface (**Figure 2**), the squared law of distance is given by **Equations 1** and **2**:

$$\frac{I_0}{I_g} = \left(\frac{SSD_{eff} + d_{max} + g}{SSD_{eff} + d_{max}}\right)^2 \quad \text{Eq. 1}$$

By having a root from this formula and some equalization, the following formula is obtained.

$$\sqrt{\frac{I_0}{I_g}} = \frac{g}{SSD_{eff} + d_{max}} + 1 \quad \text{Eq. 2}$$

Then $\sqrt{I_0/I_g}$ should be plotted versus $g$. The linear plot of $\sqrt{I_0/I_g}$ versus the gap between the applicator end and the phantom surface in cm, has a slope and this slope can be used to calculate the $SSD_{eff}$ according to **Equation 3**:

$$SSD_{eff} = \frac{1}{slope} + d_{max} \quad \text{Eq. 3}$$

More details on the squared law of distance and these formulas were described in the study by Khan et al.[9] It should be noted that in the measurement of $I_0/I_g$, measurements of both values of $I_0$ and $I_g$ doses are performed with a single detector. This quantity has not units. Therefore some conversion factors can be eliminated in the numerator and denominator of the ratio and the $I_0/I_g$ ratio can be assumed as the ratio of readings for a single detector.

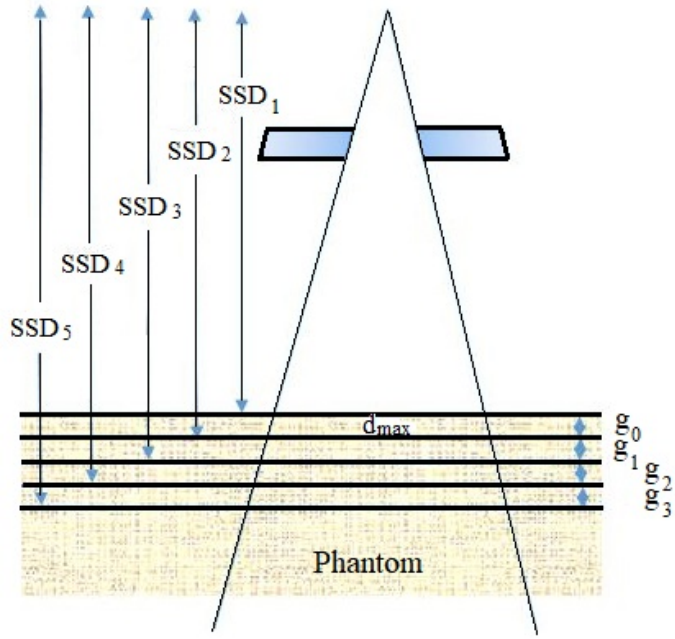


**Figure 2. A schematic illustration indicating different set ups used for measurements.**

This process was repeated for the other detectors (Semiflex 3D and Advanced Markus) by replacing them instead of the Diode E detector (using their PTW TRUFIX positioning system).

## Measurement of cutout factor

To measure the cutout factor,[9] the $d_{max}$ for each energy was first obtained, then for example the Diode E detector was placed at the corresponding $d_{max}$ in the phantom, and the absolute dose value was obtained for each field. In other words,

for each energy, the detector was set at the $d_{max}$ of the reference applicator size (6 × 6 $cm^2$) in that energy. In electron beams, the variation of the $d_{max}$ for the field sizes that have close dimensions with each other is negligible. However, $d_{max}$ was measured for different cut outs, but the results of $d_{max}$ were relatively the same.

Cutout factor was obtained for the mentioned energies according to **Equation 4**:

$$\text{Cutout factor} = \frac{D_{\text{field}}}{D_{\text{ref}}} \quad \text{Eq. 4}$$

In **Equation 4** $D_{field}$ is the dose value in each field and $D_{ref}$ is the dose value in the reference field of 6 × 6 $cm^2$. As it was mentioned before, cutout factor was obtained for small fields (up to 6×6 $cm^2$) at 100, 105, 110, 115 and 120 cm SSDs, **Figure 1** (part b). Again, cutout factors for all mentioned SSDs were measured with the two other dosimeters (Semiflex 3D and Advanced Markus) with a manner the same as the method used for Diode E detector.

## Results

As it was mentioned before, $SSD_{eff}$ and cutout factor were measured for the Elekta Precise linac by different dosimeters including a Semiflex and Advanced Markus ionization chambers and Diode E detector. Values of $\sqrt{I_0/I_g}$ for the studied fields at 100, 105, 110, 115, and 120 cm SSDs at 10, 15, and 18 MeV energies are presented in **Table 1**. The values of $SSD_{eff}$ (in cm) were obtained for the studied fields in 10, 15, and 18 MeV electron beam energies using the $\sqrt{I_0/I_g}$ values, according to **Equation 3**, and the results are listed in **Table 2**. The $SSD_{eff}$ results obtained by measurement by Semiflex and Advanced Markus ionization chambers and Diode E detector for small and large fields at 10, 15, and 18 MeV electron beam energies are also presented in **Figure 3**.

The results of the cutout factor, measured by the Semiflex and Advanced Markus ionization chambers and Diode E detector, for the small fields (up to 6×6 $cm^2$) at electron beam energies of 10, 15, and 18 MeV at 100, 105, 110, 115 and 120 cm SSDs are illustrated in **Figure 4**.

**Table 1. $\sqrt{\frac{I_0}{I_g}}$ values for different fields and SSDs at 10, 15, and 18 MeV.**

| Energy (MeV) | SSD (cm) | Field size ($cm^2$) | | | | | | | | | | | |
|---|---|---|---|---|---|---|---|---|---|---|---|---|---|
| | | 1.5×1.5 | 2×2 | 2.2×2.5 | 3×3 | 3.5×3.5 | 4×4 | 4.5×4.5 | 5×5 | 6×6 | 10×10 | 14×14 | 20×20 |
| 10 | 105 | 1.13 | 1.11 | 1.09 | 1.07 | 1.07 | 1.07 | 1.07 | 1.07 | 1.07 | 1.06 | 1.05 | 1.05 |
| | 110 | 1.28 | 1.24 | 1.19 | 1.16 | 1.14 | 1.14 | 1.14 | 1.14 | 1.13 | 1.11 | 1.11 | 1.10 |
| | 115 | 1.46 | 1.39 | 1.29 | 1.26 | 1.26 | 1.20 | 1.21 | 1.21 | 1.20 | 1.17 | 1.16 | 1.15 |
| | 120 | 1.65 | 1.55 | 1.45 | 1.36 | 1.31 | 1.30 | 1.28 | 1.28 | 1.27 | 1.22 | 1.22 | 1.21 |
| 15 | 105 | 1.08 | 1.07 | 1.06 | 1.06 | 1.06 | 1.06 | 1.06 | 1.06 | 1.06 | 1.05 | 1.05 | 1.05 |
| | 110 | 1.17 | 1.16 | 1.13 | 1.13 | 1.12 | 1.12 | 1.12 | 1.12 | 1.12 | 1.11 | 1.10 | 1.10 |
| | 115 | 1.28 | 1.25 | 1.21 | 1.20 | 1.18 | 1.18 | 1.18 | 1.18 | 1.18 | 1.16 | 1.16 | 1.15 |
| | 120 | 1.39 | 1.36 | 1.29 | 1.27 | 1.25 | 1.24 | 1.24 | 1.24 | 1.25 | 1.21 | 1.21 | 1.20 |
| 18 | 105 | 1.07 | 1.07 | 1.06 | 1.06 | 1.06 | 1.06 | 1.06 | 1.06 | 1.06 | 1.05 | 1.05 | 1.05 |
| | 110 | 1.15 | 1.14 | 1.12 | 1.12 | 1.12 | 1.12 | 1.12 | 1.12 | 1.12 | 1.11 | 1.10 | 1.10 |
| | 115 | 1.24 | 1.22 | 1.19 | 1.18 | 1.18 | 1.18 | 1.18 | 1.18 | 1.18 | 1.16 | 1.16 | 1.15 |
| | 120 | 1.33 | 1.31 | 1.27 | 1.24 | 1.23 | 1.23 | 1.23 | 1.23 | 1.23 | 1.21 | 1.21 | 1.20 |

**Table 2. Results of $SSD_{eff}$ obtained by Semiflex and Advanced Markus ionization chambers and Diode E detector in the studied fields at 10, 15, and 18 MeV electron beam energies.**

| | Field size ($cm^2$) | 10 MeV | | | 15 MeV | | | 18 MeV | | |
|---|---|---|---|---|---|---|---|---|---|---|
| | | Semiflex | Advanced Markus | Diode E | Semiflex | Advanced Markus | Diode E | Semiflex | Advanced Markus | Diode E |
| Small field, with the cutout | 1.5 ×1.5 [a] | 29.55 | 40.84 | 28.57 | 49.66 | 51.06 | 48.25 | 68.32 | 58.73 | 57.89 |
| | 2 × 2[a] | 35.21 | 50.00 | 33.77 | 55.05 | 55.72 | 53.05 | 71.47 | 64.49 | 60.97 |
| | 2.5 × 2.5[a] | 44.63 | 52.87 | 43.25 | 67.02 | 63.81 | 65.52 | 78.05 | 70.37 | 72.47 |
| | 3 × 3[a] | 54.40 | 59.65 | 53.05 | 73.34 | 72.21 | 71.56 | 84.36 | 80.02 | 77.93 |
| | 3.5 × 3.5[a] | 64.57 | 65.95 | 63.16 | 80.22 | 78.88 | 78.79 | 85.12 | 83.59 | 79.92 |
| | 4 × 4[a] | 66.87 | 68.84 | 65.37 | 80.91 | 80.91 | 80.82 | 85.90 | 84.34 | 82.03 |
| | 4.5 × 4.5[a] | 69.33 | 71.45 | 68.72 | 81.61 | 81.61 | 81.52 | 86.69 | 85.10 | 82.75 |
| | 5 × 5[a] | 70.89 | 74.84 | 70.79 | 82.33 | 82.33 | 82.24 | 87.49 | 85.88 | 83.49 |
| Large field, with the applicator | 6 × 6[b] | 74.82 | 77.92 | 72.99 | 83.79 | 83.05 | 83.70 | 88.31 | 87.47 | 85.00 |
| | 10 × 10[b] | 82.65 | 88.01 | 81.13 | 87.67 | 88.49 | 85.21 | 89.99 | 88.29 | 87.37 |
| | 14 × 14[b] | 87.99 | 90.51 | 86.30 | 91.92 | 92.82 | 90.95 | 91.74 | 90.84 | 90.74 |
| | 20 × 20[b] | 92.24 | 93.16 | 90.39 | 95.62 | 95.62 | 93.64 | 97.58 | 94.47 | 92.52 |

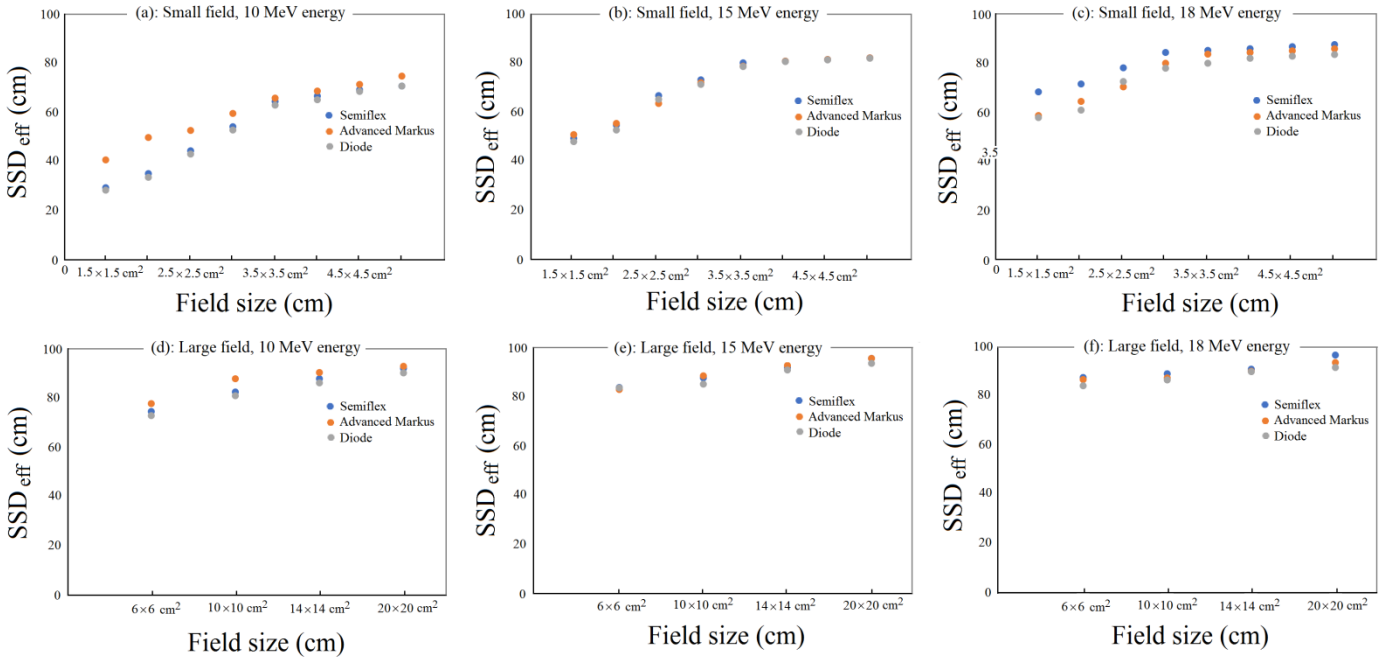


**Figure 3. Results of $SSD_{eff}$ obtained by Semiflex and Advanced Markus ionization chambers and Diode E detector for small and large fields at 10, 15, and 18 MeV electron beam energies.**

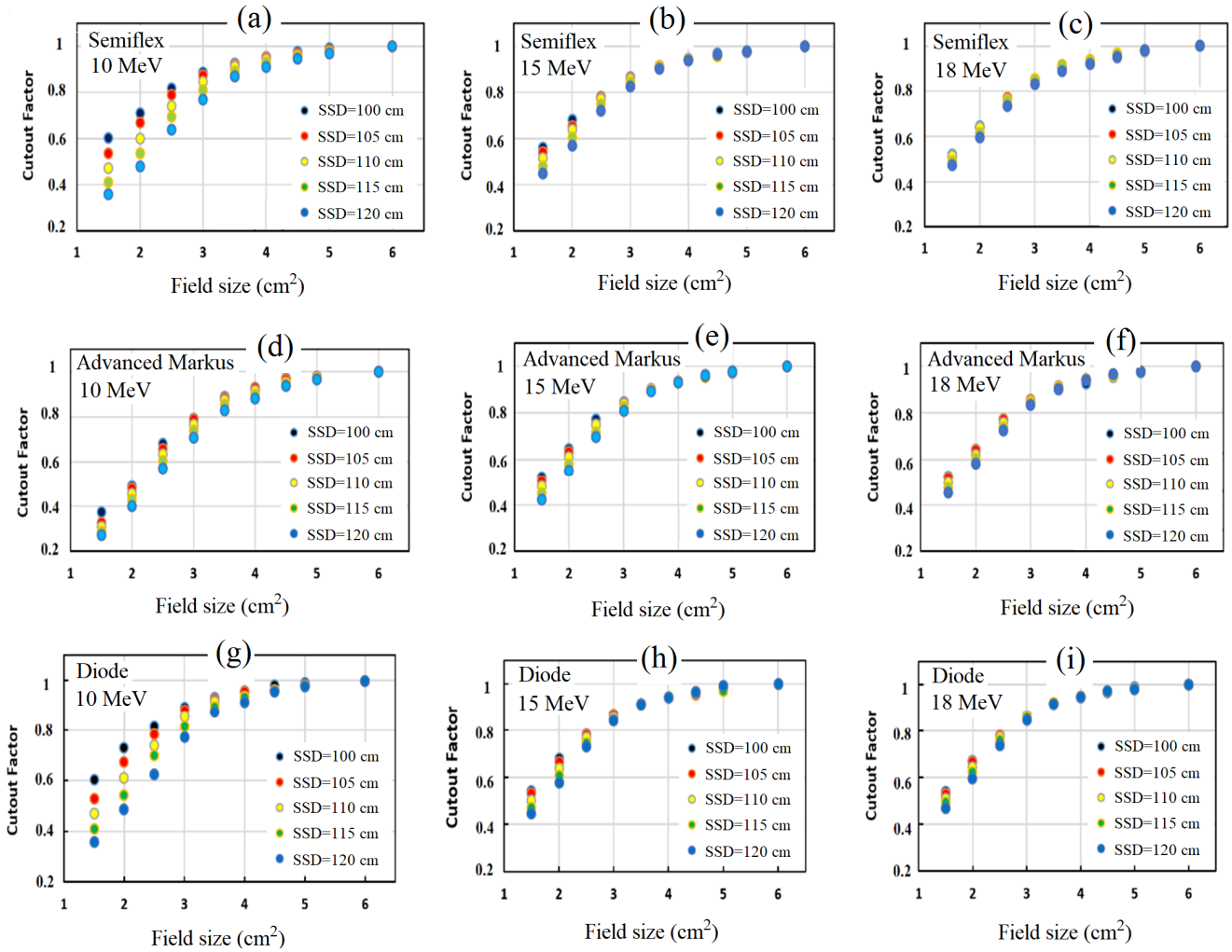


**Figure 4. Cutout factor diagram obtained by the Semiflex and Advanced Markus ionization chambers and Diode E detector, for the small fields in 10, 15 and 18 MeV electron beam energies at SSD of 100, 105, 110, 115 and 120 cm. It should be noted that 6×6 $cm^2$ field is not a small field but the other data were normalized to the data in the 6×6 $cm^2$ field.**

## Discussion

In the present study, $SSD_{eff}$ of small and large electron fields at energies of 10, 15, and 18 MeV was determined and the effect of SSD on cutout factor for small fields was evaluated for a linear accelerator. The accuracy of different dosimeters was evaluated with this regard. Based on the results in **Table 1**, in each SSD, $\sqrt{I_0/I_g}$ decreases with increasing field size. $\sqrt{I_0/I_g}$ decreases with increasing energy as well. Additionally, $\sqrt{I_0/I_g}$increases by increasing SSD in each field size and this change is greater in 10 MeV electron beam energy compared to 15 and 18 MeV energies. This change is also more dominant in the smaller square fields compared with the larger ones. The more dominant increase or decrease of this quantity shows the more effect of g on $\sqrt{I_0/I_g}$ and therefore on $SSD_{eff}$. In larger field sizes and higher energies, the changes are slower.

As it is evident from the data presented in **Table 2** and **Figure 3**, $SSD_{eff}$ is dependent on energy and field dimensions in small fields and increases with increasing field size and electron beam energy. In larger fields, these changes are less dominant, and it can be mentioned that the $SSD_{eff}$ increases with an increase in field size. For large electron fields, with some exceptions for the 20×20 $cm^2$ field, this quantity increases with energy. These effects can be due to some phenomena including: the higher number of electrons scattered from the applicator walls reaching the point of measurement in the smaller fields; the higher number of scattered electrons in a forward direction in higher energies; the higher head leakage in higher electron energies; and the difference in lateral electron equilibrium in different energies for the small field sizes.

The $SSD_{eff}$ (**Table 2** and **Figure 3**) increases with increasing field size and electron beam energy for all the three detectors (Semiflex and Advanced Markus ionization chambers and Diode E detector). This increase can be expectable for higher electron energies since higher energy electron energies are scattered more into the forward direction. A gradual increase in $SSD_{eff}$ with increasing applicator size occurs for the three detectors. This can be justified due to the scattering of electrons from the walls of the applicators. For small fields, in 10 MeV electron energy, the $SSD_{eff}$ results from measurements by Advanced Markus ionization chamber have higher values compared to Semiflex and Diode E detectors. In 15 MeV energy, for small fields with dimensions larger than 4×4 $cm^2$, this trend is not dominant. In 18 MeV electron beam energy for small fields, the values obtained by Semiflex are to some extent higher, and the values from Advanced Markus and Diode E detectors are relatively the same. For large fields, in 10 MeV energy, for the 6×6 $cm^2$ and 10×10 $cm^2$ fields, the $SSD_{eff}$ values obtained by Advanced Markus chamber is higher than Semiflex and Diode E detectors. In the case of large fields, in 15 MeV energy, the responses of the three dosimeters are relatively the same and for the 18 MeV case, they are relatively the same, but there are some minor differences in the 20×20 $cm^2$ field. The difference in the responses by these dosimeters can be due to their different sensitive volume since the sensitive volume can have an effect on special resolution. Additionally, having a smaller sensitive volume is accounted as an advantage because there is a higher probability for the existence of lateral electron equilibrium by a smaller sensitive volume of a dosimeter. In this case, being comparable to the sensitive volume and the radius required for lateral electron equilibrium is important. The sensitive volume of the Semiflex ionization chamber, Advanced Markus ionization chamber, and Diode E detector which were used for dosimetry are 0.07 $cm^3$, 0.02 $cm^3$, and 0.03 $mm^3$, respectively. Additionally, based on the specifications of these detectors, the minimum field size in which the dosimetry can be performed is 2.5×2.5 $cm^2$, 3×3 $cm^2$, and 1×1 $cm^2$, respectively.[10] Therefore, Semiflex chamber has some uncertainties 1.5×1.5 $cm^2$ and 2×2 $cm^2$ fields and the Advanced Markus for 1.5×1.5 $cm^2$, 2×2 $cm^2$, and 2.5×2.5 $cm^2$ fields. This is also expectable based on the sensitive volume of the detectors since the minimum volume is for Diode E detector. Having a smaller sensitive volume by Diode E detector is an advantage of this detector over the other two dosimeters. Therefore, for electron beam dosimetry for these field sizes (1.5×1.5 $cm^2$, 2×2 $cm^2$, and 2.5×2.5 $cm^2$) the Diode E detector can be recommended. The small fields are useful more frequently in treatments of superficial legions in head and neck cancers. On the other hand, large fields are normally used as a boost for photon beam radiotherapy on other body sites.

There are several studies that approve diode detectors for dosimetry in electron small fields, based on Monte Carlo simulations of small fields of linacs.[11] In this research it was decided to use a diode as an approved dosimeter for electron small field dosimetry. It is noticeable that diodes are routine dosimeters in small field dosimetry because of their small sensitive volume and real-time readout and high spatial resolution but diodes have some disadvantages such as dependence on energy, dose rate, and direction. Semiflex 3D is a new dosimeter for photon and electron beams that have small sensitive volume and has been designed for axial and radial beam incidence irradiations, offering greater flexibility and helping to reduce positioning errors in the measurement setups. Minimal stem and cable effects for this chamber allow high-resolution profile measurements in axial orientation. Advanced Markus chamber is also a recommended plane parallel dosimeter for electron dosimetry. The two later chambers were not recommended for small field dosimetry based on their catalogues, but they have some other advantages in electron beam dosimetry. Therefore, the results of the present study are useful for the evaluation of the advantages and disadvantages of Semiflex and Advance Markus ionization chambers in small and large field dosimetry, compared to the Diode E detector.

The results presented for these three detectors can be useful for the selection of an adequate detector for electron dosimetry in small electron fields. This condition is encountered in cases such as damage of a detector, providing a new dosimetry

system for electron dosimetry, or finishing the date of calibration of a detector in a radiotherapy department. In such cases, substituting an alternative dosimeter can be useful. While radiochromic film dosimetry and Monte Carlo simulation can be accurate for electron small field dosimetry, but these methods are time-consuming and may not be feasible in all conditions.

The diagrams in **Figure 2** for the cutout factors show that there are differences in cutout factors for different field sizes, electron energies, and dosimeters. Additionally, as the SSD increases, cutout factor decreases. By increase of field size, the cutout factor increases and it reaches to value of 1.00 at 6×6 $cm^2$, since this is the reference field and the values were normalized to this field. The difference between the cutout factors is larger in the smaller field sizes, in other words, the differences in cutout factors decrease with the increase of field size. Furthermore, and these differences are more dominant in 10 MeV electron beam energy and are less in 18 MeV energy. The cutout factors determined by different dosimeters are different, especially for small electron fields and lower electron energies. This may be due to the absence of lateral particle equilibrium in small electron fields and sensitive volume of the detectors.

Different studies[5-9,12-17] have evaluated $SSD_{eff}$ for electron beams of different models of linacs including Varian and Siemens, however, there is not any research on $SSD_{eff}$ determination of Elekta Precise linac. Therefore, the values from the present study cannot be compared with the other studies. On the other hand, comparison of the trends of $SSD_{eff}$ with a change of electron energy and field size is useful.

AAPM in the report by Task Group number 25 (TG25), has recommendations on electron beam dosimetry, especially for small electron fields.[3] Based on this report, due to inherent problems in the existence of electron equilibrium in small electron fields, custom measurements should be performed to determine the change in dose distributions in small electron fields. The custom measurements and the dosimetry data presented in this study cannot be used by other radiotherapy departments for Elekta Precise linac, since the dosimetry data are linac specific. However, they can be used as a guide or overall estimation of dosimetry data for electron beams of Elekta Precise linac. Following the recommendations by TG25 and the supplement to TG25 report[18] has illuminating points in the field of electron beam dosimetry.

As it is evident from the results, there are differences in the values of $SSD_{eff}$ and cutout factors for small fields determined by different dosimeters. A comparison of the results with corresponding measurements with radiochromic film, diamond dosimeters, or Monte Carlo simulation could be useful to determine the dosimeter with more accurate values. Diamond and radiochromic film dosimeters with smaller sensitive volumes have a better special resolution in this regard. While radiochromic film dosimetry and Monte Carlo simulation can be accurate for electron small field dosimetry, but these methods are time-consuming and may not be feasible in all conditions. Additionally, the Elekta Precise linac normally has 6 and 8 MeV electron beams. While in the present study those energies with more clinical applications (10, 15, and 18 MeV) were selected, these energies were not evaluated. These subjects can be useful for further research in the field of electron beam dosimetry as future studies.

It would be useful if the Monte Carlo simulation was used in this study as reference dosimetry for small electron beams and if the results were compared with the measurements. Monte Carlo simulation of a linac requires the geometry of the linac and validation of linac simulation. This was not performed in this study due to the lack of geometry information and is accounted for as a limitation of this study. However, this is suggested as a subject on more evaluations in this field. In the present study, the results of the diode E dosimeter can be accounted as the reference. Diode detectors, due to small sizes, can be used as reference dosimeters in small field dosimetry and were utilized in a number of previous studies on this subject. It is noticeable that diodes are routine dosimeters in small field dosimetry because of their small sensitive volume and real-time readout and high spatial resolution but they have disadvantages such as dependence on energy, dose rate, and direction.[19-20]

## Conclusion

The evaluations of this study on $SSD_{eff}$ for different electron field sizes and energies indicate that $SSD_{eff}$ varies significantly between different fields specified by electron applicators and cutouts. $SSD_{eff}$ is highly dependent on electron beam energy and field size in small fields and increases with increasing field and electron beam energy. For large electron fields, with some exceptions for the 20×20 $cm^2$ field, this quantity also increases with energy. There are differences in $SSD_{eff}$ and cutout factors determined by different dosimeters in small fields especially at lower electron energies. Having a smaller sensitive volume by Diode E detector is an advantage of this detector over the other two dosimeters and for electron beam dosimetry for 1.5×1.5 $cm^2$, 2×2 $cm^2$, and 2.5×2.5 $cm^2$ field sizes, the Diode E detector can be recommended as the reference dosimeter in small field dosimetry, compared to the other two dosimeters. Selecting the appropriate dosimetric system can be effective in determining the cutout factor in electron beam radiotherapy. The results presented herein can be useful for the selection of an adequate detector for electron dosimetry in small electron fields. It is recommended that the $SSD_{eff}$ be determined for each electron field when treatment is performed with partially blocked electron fields shaped with electron cutouts.

## Acknowledgment

The authors would like to thank Kashan University of Medical Sciences and the Department of Radiotherapy and Oncology of Ayatollah Khansari Hospital (Arak, Iran) for the financial and technical support of this work. This study was supported with a grant number of 1232 and an ethical code of IR.ARAKMU.REC.1395.223.

## References

1. ICRU. ICRU Report No. 35. Electron beams with energies between 1 and 50 MeV. ICRU, Bethesda, 1984.
2. Khan FM, Sewchand W, Levitt SH. Effect of air space on depth dose in electron beam therapy. Radiology 1978;126(1):249-51.
3. Amin MN, Heaton R, Norrlinger B, Islam MK. Small field electron beam dosimetry using MOSFET detector. J Appl Clin Med Phys 2010,12(1):50-57.
4. Khan FM, Doppke KP, Hogstrom KR, Kutcher GJ, Nath R, Prasad SC, et al. Clinical electron beam dosimetry: Report of AAPM Radiation Therapy Committee Task Group No. 25. Med Phys 1991;18,73-109.
5. Jamshidi A, Kuchnir FT, Reft CS. Determination of the source position for the electron beams from a high-energy linear accelerator. Med Phys 1986;13(6):942-8.
6. Al Asmary M, Ravikumar M. Position of effective electron source for shielded electron beams from a therapeutic linear accelerator. Pol J Med Phys Engin 2010;16(1):11-21.
7. Shafaei Douk HS, Aghamiri MR, Ghorbani M, Farhood B, Bakhshandeh M, Hemmati HR. Accuracy evaluation of distance inverse square law in determining virtual electron source location in Siemens Primus linac. Rep Pract Oncol Radiother 2018;23(2):105-13.
8. Tahmasebi Birgani MJ. Zabihzadeh M, Arvandi Sh. Gharibreza E. Determining the effective source-surface distance for therapeutic electron beams. Jentashapir J Health Res 2016;7(3):30975.
9. Khan FM, Sewchand W, Levitt SH. Effect of air space and depth dose in electron beam therapy. Radiology 1978;126(1):249-51.
10. PTW The dosimetry company Available at: https://www.ptwdosimetry.com/en/support/downloads/?type=3451&downloadfile=1503. Accessed on: 6/3/2020.
11. Björk P, Knöös T, Nilsson P. Measurements of output factors with different detector types and Monte Carlo calculations of stopping-power ratios for degraded electron beams. Phys Med Biol 2004;49(19):4493-506.
12. Hu YA, Song H, Chen Z, Zhou S, Yin FF. Evaluation of an electron Monte Carlo dose calculation algorithm for electron beam. J Appl Clin Med Phys 2008;9(3):2720.
13. Lief EP, Lutz WR. Determination of effective electron source size using multislit and pinhole cameras. Med Phys 2000;27:2372-5.
14. Roback DM, Khan FM, Gibbons JP, Sethi A. Effective SSD for electron beams as a function of energy and beam collimation. Med Phys 1995;22:2093-5
15. Sharma SC, Johnson MW. Electron beam effective source surface distances for a high energy linear accelerator. Med Dosim 1991;16:65-70.
16. Ghasemi H, Azma Z, Jabbary Arfaee A, Sadeghi M. Verification of Experimental Virtual Electron Source Position by Using Monte Carlo. Res Rev: J Pure Appl Phys 2018;6:9-16.
17. Papatheodorou S, Malatara G. Electron beam output of an Elekta Sli-Plus linear accelerator for irregular shaped fields and for extended SSD. Phys Med 2016;32:284-339.
18. Gerbi BJ, Antolak JA, Deibel FC, Followill DS, Herman MG, Higgins PD, et al. Recommendations for clinical electron beam dosimetry: supplement to the recommendations of Task Group 25. Med Phys 2009;36:3239-79.
19. Keivan H, Shahbazi-Gahrouei D, Shanei A. Evaluation of dosimetric characteristics of diodes and ionization chambers in small megavoltage photon field dosimetry. Int J Radiat Res 2018, 16(3): 311-321
20. Saidani I, Ben Salem L, Besbes M. Small field dosimetry for electron beams using four types of detectors. Phys Med 2018; 56(1):55